





Ornstein-Uhlenbeck information swimmers with external and internal feedback controls

ZHANGLIN HOU^{1,2} , ZILUO ZHANG^{1,3} , JUN LI^{4,1}, KENTO YASUDA⁵  and SHIGEYUKI KOMURA^{1,2(a)} 

¹ Wenzhou Institute, University of Chinese Academy of Sciences - Wenzhou, Zhejiang 325001, China

² Oujiang Laboratory - Wenzhou, Zhejiang 325000, China

³ Institute of Theoretical Physics, Chinese Academy of Sciences - Beijing 100190, China

⁴ Department of Physics, Wenzhou University - Wenzhou, Zhejiang 325035, China

⁵ Research Institute for Mathematical Sciences, Kyoto University - Kyoto 606-8502, Japan

received 19 January 2025; accepted in final form 25 March 2025
published online 28 April 2025

Abstract – Using an underdamped active Ornstein-Uhlenbeck particle, we propose two information swimmer models having either external or internal feedback control and perform their numerical simulations. Depending on the velocity that is measured after every fixed time interval (measurement time), the friction coefficient is modified in the externally controlled model, whereas the persistence time for the activity is changed in the internally controlled one. In the steady state, both of these information swimmers acquire finite average velocities in the noisy environment, and their efficiencies can be maximized by tuning the measurement time. The internally controlled swimmer can generally achieve a larger velocity and efficiency than the externally controlled one when the active fluctuation is large.



Copyright © 2025 The author(s)

Published by the EPLA under the terms of the [Creative Commons Attribution 4.0 International License](https://creativecommons.org/licenses/by/4.0/) (CC BY). Further distribution of this work must maintain attribution to the author(s) and the published article's title, journal citation, and DOI.

Introduction. – In the studies of active matter, much interest has been focused on the collective motions of self-propelled particles [1]. It is also important to understand the mechanism of single-particle motion from the perspective of non-equilibrium statistical mechanics [2]. Among various models, the self-propulsion of an active Brownian particle (ABP) is generated by an internal driving force combined with overdamped orientational Brownian dynamics [3]. An overdamped self-propelled motion can be described by an active Ornstein-Uhlenbeck particle (AOUP) driven by a stochastic force whose memory decays exponentially in time [4]. Since the AOUP model exhibits persistent particle motion mimicking the activity, it offers a basic reference for active dynamics of cells and bacteria [5].

Although both ABP and AOUP are active, they undergo Brownian dynamics in the long time limit [6] and cannot have any net locomotion on average. For microswimmers in a Newtonian fluid, it is known that non-reciprocal cyclic body motion is required for their persistent locomotion [7,8]. To maintain such continuous movement, a constant supply of mechanical energy and

its dissipation to the surrounding fluid is necessary [9]. Other active systems driven by energy injection include Janus particles that consume a chemical fuel [10]. In contrast to these microswimmers, the “odd microswimmer” consisting of three spheres and two odd springs is purely driven by thermal energy of the surrounding fluid [11,12].

Recently, much attention has been paid to active systems that utilize information instead of energy, *i.e.*, informational active matter [13]. During the last decade, there have been many studies on “information engines” that use information to extract mechanical work [14–16]. One example proposed by Huang *et al.* is the “information swimmer” in which the swimmer periodically measures its velocity and adjusts its friction coefficient [17]. They showed that the information swimmer can achieve a steady-state velocity without external energy input, which is consistent with the extended second law of thermodynamics with information [18]. This model can also be regarded as one type of “information ratchet” that leads to directional transport or locomotion by repeating measurements and feedback controls [19,20].

In the absence of measurement and feedback, the information swimmer proposed by Huang *et al.* [17] is passive

^(a)E-mail: komura@wiucas.ac.cn (corresponding author)

and purely governed by thermal fluctuations. From the viewpoint of informational active matter [13], however, it is of interest to consider a swimmer that controls its internal activity depending on the measurement result. In this letter, we propose models of information swimmers by using an underdamped AOUP and call them “Ornstein-Uhlenbeck information swimmers” (OUIs). To highlight the role of activity, we discuss two different models: i) OUIS with *external* feedback control (E-OUIS) and ii) OUIS with *internal* feedback control (I-OUIS). Depending on the particle velocity, the friction coefficient is adjusted in the E-OUIS (similar to ref. [17]), whereas the persistence time for the activity is controlled in the I-OUIS. While the externally controlled swimmer requires some structural changes in volume or shape [17], the internal control can be achieved by various chemical and mechanical processes [21], such as the run-and-tumble motion of *Escherichia coli* [22,23]. We perform numerical simulations of the two models and discuss their swimming performance. Although both OUIS models can maintain a steady motion, the I-OUIS can generally achieve a larger velocity and efficiency than the E-OUIS when the active fluctuation becomes large.

OUIS with external feedback control (E-OUIS).

– We consider an underdamped AOUP moving in a one-dimensional space [24,25]. In the E-OUIS model, the AOUP measures its center-of-mass velocity v after every time interval τ_m (measurement time) and compares it with a threshold velocity v_0 [17,26]. The friction coefficient is set to be $\alpha_1^2\Gamma$ and $\alpha_2^2\Gamma$ if $v \leq v_0$ and $v > v_0$, respectively, where α_1 and α_2 are dimensionless coefficients and we typically choose $\alpha_1 > \alpha_2$. The change in the friction coefficient can be induced by some structural changes, such as the particle volume, shape, and surface structure [17]. The results of measurement are recorded in the swimmer’s internal memory that is assumed to be sufficiently large.

During the time interval $n\tau_m < t < (n+1)\tau_m$, the Langevin equation for the underdamped E-OUIS is given by

$$M\dot{v}(t) = \begin{cases} -\alpha_1^2\Gamma[v(t) - u(t)] + \alpha_1\sqrt{2\Gamma k_B T}\zeta(t), & v(n\tau_m) \leq v_0, \\ -\alpha_2^2\Gamma[v(t) - u(t)] + \alpha_2\sqrt{2\Gamma k_B T}\zeta(t), & v(n\tau_m) > v_0. \end{cases} \quad (1)$$

Here, M is the particle mass, $\dot{v} = dv/dt$, Γ is the friction coefficient, k_B is the Boltzmann constant, T is the temperature, and $\zeta(t)$ is the Gaussian white noise with zero mean and unit variance:

$$\langle \zeta(t) \rangle = 0, \quad \langle \zeta(t)\zeta(t') \rangle = \delta(t - t'). \quad (2)$$

The coefficients of the noise terms in eq. (1) are chosen to satisfy the fluctuation-dissipation relation for both $v \leq v_0$ and $v > v_0$, reflecting the equilibrium nature of the ambient environment [27]. Note that the threshold velocity v_0

can take both positive and negative values. In the above, we assume that the change of the friction coefficient does not require any mechanical work [17].

In eq. (1), u is a stochastic driving velocity with memory on a finite time leading to a persistent motion [24,25]. It mimics the activity of the particle and evolves through an Ornstein-Uhlenbeck process [4],

$$\dot{u}(t) = -\frac{u(t)}{\tau_a} + \frac{\sqrt{2A}}{\tau_a}\xi(t), \quad (3)$$

where τ_a is the persistence time, A is the strength of active fluctuation (having the dimension of a diffusion constant). The term $\xi(t)$ in eq. (3) also represents the Gaussian white noise with zero mean and unit variance:

$$\langle \xi(t) \rangle = 0, \quad \langle \xi(t)\xi(t') \rangle = \delta(t - t'). \quad (4)$$

Although we do not discuss here the chemical or mechanical origins of the driving velocity u , it pushes the particle away from equilibrium and guarantees a persistent motion in one direction for times smaller than τ_a . The parameters τ_a and A can be used to quantify the activity of the AOUP, such as the persistence length $\ell_0 = \sqrt{A\tau_a}$ and the magnitude of the driving velocity $u_0 = \sqrt{A/\tau_a}$ [24,25].

In the following analysis, we use the Brownian relaxation time $\tau = M/\Gamma$ and the thermal velocity $v_T = \sqrt{k_B T/M}$ to rescale the variables as $\tilde{t} = t/\tau$, $\tilde{v}(\tilde{t}) = v(t)/v_T$, $\tilde{u}(\tilde{t}) = u(t)/v_T$, $\tilde{\zeta}(\tilde{t}) = \sqrt{2M/\Gamma}\zeta(t)$, and $\tilde{\xi}(\tilde{t}) = \sqrt{2M/\Gamma}\xi(t)$. Moreover, the dimensionless parameters are defined as $\tilde{\tau}_m = \tau_m/\tau$, $\tilde{v}_0 = v_0/v_T$, $\tilde{\tau}_a = \tau_a/\tau$, and $\tilde{A} = A\Gamma/(k_B T)$. Then, the dimensionless form of the E-OUIS model can be summarized as

$$\frac{d\tilde{v}(\tilde{t})}{d\tilde{t}} = \begin{cases} -\alpha_1^2[\tilde{v}(\tilde{t}) - \tilde{u}(\tilde{t})] + \alpha_1\tilde{\zeta}(\tilde{t}), & \tilde{v}(n\tilde{\tau}_m) \leq \tilde{v}_0, \\ -\alpha_2^2[\tilde{v}(\tilde{t}) - \tilde{u}(\tilde{t})] + \alpha_2\tilde{\zeta}(\tilde{t}), & \tilde{v}(n\tilde{\tau}_m) > \tilde{v}_0, \end{cases} \quad (5)$$

$$\frac{d\tilde{u}(\tilde{t})}{d\tilde{t}} = -\frac{\tilde{u}(\tilde{t})}{\tilde{\tau}_a} + \frac{\sqrt{\tilde{A}}}{\tilde{\tau}_a}\tilde{\xi}(\tilde{t}), \quad (6)$$

$$\langle \tilde{\zeta}(\tilde{t}) \rangle = 0, \quad \langle \tilde{\zeta}(\tilde{t})\tilde{\zeta}(\tilde{t}') \rangle = 2\delta(\tilde{t} - \tilde{t}'), \quad (7)$$

$$\langle \tilde{\xi}(\tilde{t}) \rangle = 0, \quad \langle \tilde{\xi}(\tilde{t})\tilde{\xi}(\tilde{t}') \rangle = 2\delta(\tilde{t} - \tilde{t}'), \quad (8)$$

for $n\tilde{\tau}_m < \tilde{t} < (n+1)\tilde{\tau}_m$.

When $\alpha_1 = \alpha_2 = 1$, namely, when the feedback control is absent, one can easily convert the above Langevin equations to a Fokker-Planck equation and obtain the velocity autocorrelation function of an AOUP, as explained in the Supplementary Material [Supplementarymaterial.pdf](#) (SM). Using the equal-time velocity correlation, one can define the effective temperature of an AOUP as $k_B T^* = M\langle v^2 \rangle$, where

$$k_B T^* = k_B T + \frac{A\Gamma\tau}{\tau + \tau_a} = k_B T \left(1 + \frac{\tilde{A}}{1 + \tilde{\tau}_a} \right). \quad (9)$$

Hence, the effective temperature T^* is larger than T , and the additional term is proportional to the active fluctuation strength A . In the absence of feedback control

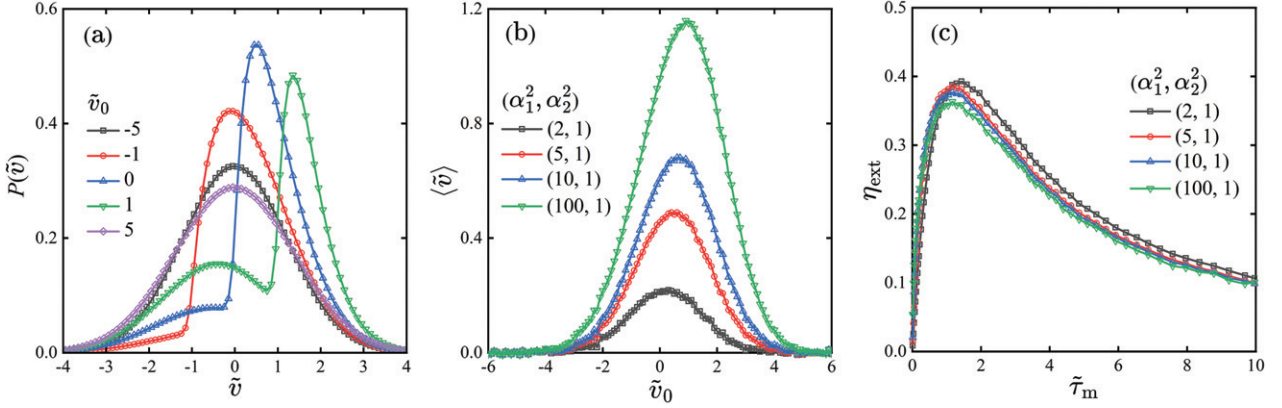


Fig. 1: Various statistical properties of the E-OUIS model with external feedback control (see eqs. (5)–(8)). The fixed parameters are $\tilde{\tau}_a = 1$ and $\tilde{A} = 1$. (a) The steady-state velocity distribution function $P(\tilde{v})$ when the threshold velocity is changed within the range of $-5 \leq \tilde{v}_0 \leq 5$. Here, we choose $(\alpha_1^2, \alpha_2^2) = (10, 1)$ and the measurement time interval is $\tilde{\tau}_m = 0.01$. (b) The steady-state average velocity $\langle \tilde{v} \rangle$ as a function of the threshold velocity \tilde{v}_0 when $(\alpha_1^2, \alpha_2^2) = (2, 1), (5, 1), (10, 1), (100, 1)$ and $\tilde{\tau}_m = 0.01$. (c) The efficiency η_{ext} of the E-OUIS model (see eq. (10)) as a function of $\tilde{\tau}_m$ for the same combinations of (α_1^2, α_2^2) shown in (b). The threshold velocity is $\tilde{v}_0 = 0$.

($\alpha_1 = \alpha_2$), however, the E-OUIS does not exhibit any net locomotion in the long time limit, as mentioned before.

The above stochastic equations for the E-OUIS are discretized over the small time step $\Delta\tilde{t} = 0.001$, and they are numerically integrated by using the first-order Euler-Maruyama scheme [28]. Among several model parameters, we fix $\tilde{\tau}_a = 1$ and $\tilde{A} = 1$, while we change α_1^2 , α_2^2 , $\tilde{\tau}_m$, and \tilde{v}_0 . When the particle has reached the steady state after 10^7 time steps, we obtain the time-independent velocity distribution function $P(\tilde{v})$ to calculate the steady-state average velocity $\langle \tilde{v} \rangle = \int_{-\infty}^{\infty} d\tilde{v} \tilde{v} P(\tilde{v})$. On the other hand, the steady-state distribution function $P(\tilde{u})$ of the driving velocity u is purely Gaussian (see eqs. (6) and (8)), and its average should vanish, $\langle \tilde{u} \rangle = 0$, as we have checked numerically.

In fig. 1(a), we show the results of the velocity distribution function $P(\tilde{v})$ of the E-OUIS when $(\alpha_1^2, \alpha_2^2, \tilde{\tau}_m) = (10, 1, 0.01)$ (corresponding to $\tilde{\tau}_m = 10\Delta\tilde{t}$) and \tilde{v}_0 is varied between $-5 \leq \tilde{v}_0 \leq 5$. When the absolute value of \tilde{v}_0 is as large as $|\tilde{v}_0| \approx 5$, $P(\tilde{v})$ is almost Gaussian and $\langle \tilde{v} \rangle$ vanishes. For $|\tilde{v}_0| < 4$, however, $P(\tilde{v})$ becomes highly asymmetric and even bimodal for $\tilde{v}_0 > 0$ (see later discussion for its physical origin). In such a situation, the average velocity is finite, $\langle \tilde{v} \rangle > 0$, and hence the E-OUIS model acquires net locomotion under noisy environment. In fig. 1(b), we plot $\langle \tilde{v} \rangle$ as a function of \tilde{v}_0 for different values of α_1^2 . The maximum of $\langle \tilde{v} \rangle$ increases for larger α_1^2 , and it occurs at positive \tilde{v}_0 such as at $\tilde{v}_0 \approx 0.6$ when $\alpha_1^2 = 10$. Notice that the induced average velocity is the order of thermal velocity v_T .

Next, we argue the swimming performance of the E-OUIS model. First, the change rate of information entropy is given by $\dot{I} = I/\tau_m$, where I is the mutual information [18]. Since there is no error in the measurement, the mutual information is equal to the Shannon entropy, $I = -k_B \sum_i p_i \ln p_i$, where p_i is the probability of the state $i = 1, 2$ and satisfies $\sum_i p_i = 1$. We have assumed that the swimmer's memory space is

sufficiently large so that the information entropy can increase steadily, and hence there is no need to erase information [17]. Second, we estimate the power of the swimmer by the product of the frictional force $\alpha_i^2 \Gamma \langle v - u \rangle_i$ and the center-of-mass velocity $\langle v \rangle_i$, and then averaged over the two states $i = 1, 2$. Dividing the average power by the effective temperature T^* in eq. (9), we estimate the entropy production rate due to the frictional motion by $\dot{\sigma}_v = \sum_i \alpha_i^2 \Gamma \langle v - u \rangle_i \langle v \rangle_i p_i / T^*$. Then, we define the entropic efficiency of the E-OUIS model as

$$\eta_{\text{ext}} = \frac{\dot{\sigma}_v}{\dot{I}} = \frac{\sum_i \alpha_i^2 \langle \tilde{v} - \tilde{u} \rangle_i \langle \tilde{v} \rangle_i p_i / \tilde{T}^*}{\tilde{I} / \tilde{\tau}_m}, \quad (10)$$

where $\tilde{T}^* = T^*/T$ and $\tilde{I} = I/k_B$. Huang *et al.* considered a similar efficiency for an information swimmer that can maintain directional motion only by measurement and feedback [17].

The above efficiency η_{ext} is plotted as a function of $\tilde{\tau}_m$ in fig. 1(c) when $\tilde{v}_0 = 0$. The overall behavior is similar for different choices of α_1^2 . The efficiency is low for small and large $\tilde{\tau}_m$ values, taking a maximum value $\eta_{\text{ext}} \approx 0.38$ at around $\tilde{\tau}_m \approx 1$ for all α_1^2 . In other words, the efficiency is maximized when the measurement time is close to the Brownian relaxation time τ . As separately shown in fig. S1 of the SM, the velocity distribution $P(\tilde{v})$ for $\tilde{\tau}_m = 1$ is more symmetric and $\langle \tilde{v} \rangle$ is smaller than that for $\tilde{\tau}_m = 0.01$. However, since \dot{I} is also smaller for $\tau_m = 1$, η_{ext} is also maximized at around $\tilde{\tau}_m \approx 1$. We have further checked the other cases of $(\alpha_2^2, \tilde{\tau}_m) = (0.1, 0.01)$ and systematically changed α_1^2 , as shown in fig. S2 in the SM. The results are similar to those in fig. 1, showing a robust dependence on the model parameters. However, as shown in fig. S2(c) in the SM, η_{ext} decreases much slower when τ_m is made larger.

OUIS with internal feedback control (I-OUIS).

– In the previous E-OUIS model, the friction coefficient

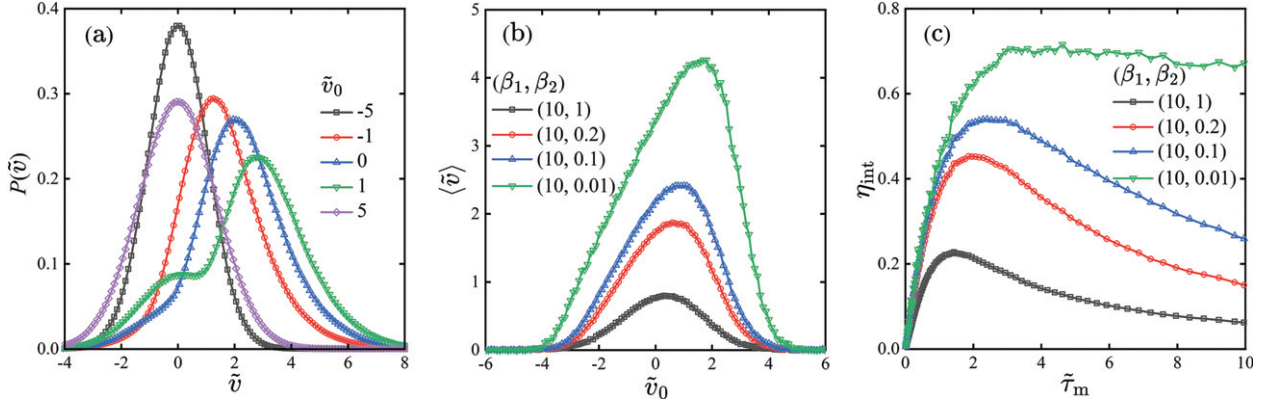


Fig. 2: Various statistical properties of the I-OUIS model with internal feedback control (see eqs. (13)–(16)). The fixed parameters are $\tilde{\tau}_a = 1$ and $\tilde{A} = 1$. (a) The steady-state velocity distribution function $P(\tilde{v})$ when the threshold velocity is changed within the range of $-5 \leq \tilde{v}_0 \leq 5$. Here, we choose $(\beta_1, \beta_2) = (10, 0.1)$ and the measurement time interval is $\tilde{\tau}_m = 0.01$. (b) The steady-state average velocity $\langle \tilde{v} \rangle$ as a function of the threshold velocity \tilde{v}_0 when $(\beta_1, \beta_2) = (10, 1)$, $(10, 0.2)$, $(10, 0.1)$, $(10, 0.01)$ and $\tilde{\tau}_m = 0.01$. (c) The efficiency η_{int} of the I-OUIS model (see eq. (17)) as a function of $\tilde{\tau}_m$ for the same combinations of (β_1, β_2) shown in (b). The threshold velocity is $\tilde{v}_0 = 0$.

of the AOUP was switched according to the measurement (see eq. (1)). Next, we consider a different type of OUIS that changes the dynamics of the driving velocity u by measuring the center-of-mass velocity v , *i.e.*, OUIS with internal feedback control (I-OUIS). With the same notation as before, the underdamped equation for an AOUP is given by

$$M\dot{v}(t) = -\Gamma[v(t) - u(t)] + \sqrt{2\Gamma k_B T}\zeta(t), \quad (11)$$

where the Gaussian white noise $\zeta(t)$ satisfies the same statistical properties as in eq. (2). In the I-OUIS model, the driving velocity u obeys either of the following equations depending on v after every time interval τ_m :

$$\dot{u}(t) = \begin{cases} -\frac{\beta_1 u(t)}{\tau_a} + \frac{\beta_1 \sqrt{2A}}{\tau_a} \xi(t), & v(n\tau_m) \leq v_0, \\ -\frac{\beta_2 u(t)}{\tau_a} + \frac{\beta_2 \sqrt{2A}}{\tau_a} \xi(t), & v(n\tau_m) > v_0. \end{cases} \quad (12)$$

Here, β_1 and β_2 are dimensionless coefficients and $\xi(t)$ also represents the Gaussian white noise as in eq. (4). Different values for β_1 and β_2 (typically chosen as $\beta_1 > \beta_2$) give rise to the internal feedback control of the swimmer. The dimensionless form of the I-OUIS model can be summarized as

$$\frac{d\tilde{v}(\tilde{t})}{d\tilde{t}} = -[\tilde{v}(\tilde{t}) - \tilde{u}(\tilde{t})] + \tilde{\zeta}(\tilde{t}), \quad (13)$$

$$\frac{d\tilde{u}(\tilde{t})}{d\tilde{t}} = \begin{cases} -\frac{\beta_1 \tilde{u}(\tilde{t})}{\tilde{\tau}_a} + \frac{\beta_1 \sqrt{\tilde{A}}}{\tilde{\tau}_a} \tilde{\xi}(\tilde{t}), & \tilde{v}(n\tilde{\tau}_m) \leq \tilde{v}_0, \\ -\frac{\beta_2 \tilde{u}(\tilde{t})}{\tilde{\tau}_a} + \frac{\beta_2 \sqrt{\tilde{A}}}{\tilde{\tau}_a} \tilde{\xi}(\tilde{t}), & \tilde{v}(n\tilde{\tau}_m) > \tilde{v}_0, \end{cases} \quad (14)$$

$$\langle \tilde{\zeta}(\tilde{t}) \rangle = 0, \quad \langle \tilde{\zeta}(\tilde{t}) \tilde{\zeta}(\tilde{t}') \rangle = 2\delta(\tilde{t} - \tilde{t}'), \quad (15)$$

$$\langle \tilde{\xi}(\tilde{t}) \rangle = 0, \quad \langle \tilde{\xi}(\tilde{t}) \tilde{\xi}(\tilde{t}') \rangle = 2\delta(\tilde{t} - \tilde{t}'). \quad (16)$$

In figs. 2(a) and (b), we plot the velocity distribution function $P(\tilde{v})$ and the velocity $\langle \tilde{v} \rangle$ of the I-OUIS, respectively, when $(\beta_1, \beta_2, \tilde{\tau}_m) = (10, 0.1, 0.01)$ for different values of \tilde{v}_0 . Similar to the E-OUIS model, $P(\tilde{v})$ becomes asymmetric with the internal feedback control, and $\langle \tilde{v} \rangle$ becomes finite. Compared to fig. 1(b), however, $\langle \tilde{v} \rangle$ is much larger when β_2 is made smaller, and reaches up to $\langle \tilde{v} \rangle \approx 4$ when $(\beta_1, \beta_2) = (10, 0.01)$ as \tilde{v}_0 is varied. In contrast to the E-OUIS case, the distribution function $P(\tilde{u})$ of the driving velocity u is no longer Gaussian and becomes highly asymmetric, as shown in fig. S3(a) in the SM. Even though $P(\tilde{v})$ and $P(\tilde{u})$ are very different in the steady state, we have numerically confirmed that the corresponding average velocities coincide, $\langle \tilde{v} \rangle = \langle \tilde{u} \rangle$ (see fig. 2(b) and fig. S3(b) in the SM). Although this is expected from eqs. (11) and (13), the variances of $P(\tilde{v})$ and $P(\tilde{u})$ plotted in figs. S3(c) and (d) in the SM, respectively, are apparently different. The results of $P(\tilde{v})$ and $\langle \tilde{v} \rangle$ with a larger measurement time $\tilde{\tau}_m = 1$ are shown in figs. S4(a) and (b) in the SM, respectively.

To discuss the efficiency of the I-OUIS model, we additionally need to take into account the active power due to the driving velocity u because its average $\langle \dot{u} \rangle$ is nonzero (unlike the E-OUIS model). Similar to the entropy production rate $\dot{\sigma}_v$ of the E-OUIS model, the active power is estimated by $\dot{W}_u = \sum_i (\beta_i M/\tau_a) \langle \dot{u} \rangle_i^2 p_i / T_i^*$, where $T_i^* = T[1 + \tilde{A}/(1 + \tilde{\tau}_a/\beta_i)]$ ($i = 1, 2$) (see eq. (9)). Notice that the effective friction for u is given here by $\beta_i M/\tau_a$ that is proportional to the mass. Using these quantities, we consider the following modified efficiency for the I-OUIS model:

$$\eta_{\text{int}} = \frac{\dot{\sigma}_v}{\dot{I} + \dot{W}_u} = \frac{\sum_i \langle \tilde{v} - \tilde{u} \rangle_i \langle \tilde{v} \rangle_i p_i / \tilde{T}_i^*}{(\tilde{I}/\tilde{\tau}_m) + \sum_i (\beta_i / \tilde{\tau}_a) \langle \tilde{u} \rangle_i^2 p_i / \tilde{T}_i^*}, \quad (17)$$

where $\tilde{T}_i^* = T_i^*/T$.

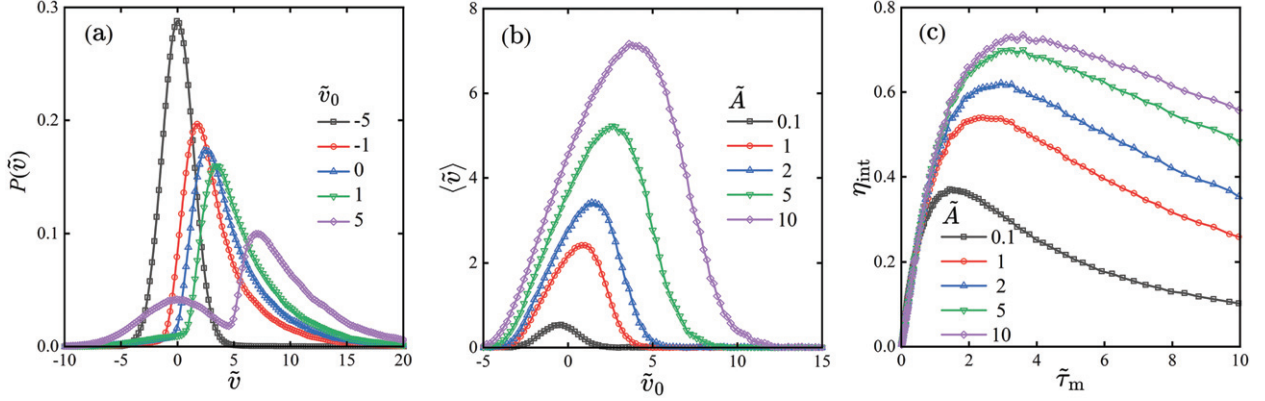


Fig. 3: Various statistical properties of the I-OUIS model with internal feedback control (see eqs. (13)–(16)). The fixed parameters are $\tilde{\tau}_a = 1$ and $(\beta_1, \beta_2) = (10, 0.1)$. (a) The steady-state velocity distribution function $P(\tilde{v})$ when the threshold velocity is changed within the range of $-5 \leq \tilde{v}_0 \leq 5$. Here, we choose $\tilde{A} = 10$ and the measurement time interval is $\tilde{\tau}_m = 0.01$. (b) The steady-state average velocity $\langle \tilde{v} \rangle$ as a function of the threshold velocity \tilde{v}_0 when $\tilde{A} = 0.1, 1, 2, 5, 10$ and $\tilde{\tau}_m = 0.01$. (c) The efficiency η_{int} of the I-OUIS model (see eq. (17)) as a function of $\tilde{\tau}_m$ for the same values of \tilde{A} shown in (b). The threshold velocity is $\tilde{v}_0 = 0$.

The above efficiency η_{int} is plotted as a function of $\tilde{\tau}_m$ in fig. 2(c) when $\tilde{v}_0 = 0$. In the case of $(\beta_1, \beta_2) = (10, 1)$, for example, the efficiency takes a maximum value $\eta_{\text{int}} \approx 0.23$ at around $\tilde{\tau}_m \approx 1.43$. When β_2 is decreased to $(\beta_1, \beta_2) = (10, 0.01)$, the efficiency increases significantly up to $\eta_{\text{int}} \approx 0.72$, and it decays slowly even for large $\tilde{\tau}_m$ values. In fig. S5 in the SM, we have performed the simulation of the I-OUIS with the other choices of parameters for which we have fixed $(\beta_1, \tilde{\tau}_m) = (1, 0.01)$ and systematically changed β_2 . The overall behavior is robust to the parameter choice as long as τ_a and \tilde{A} are fixed.

So far, the strength of active fluctuation in eq. (14) has been fixed to $\tilde{A} = 1$. Choosing $(\beta_1, \beta_2, \tilde{\tau}_m) = (10, 0.1, 0.01)$ as before, we plot in figs. 3(a), (b) and (c) the distribution function $P(\tilde{v})$, the velocity $\langle \tilde{v} \rangle$, and the efficiency η_{int} , respectively, when \tilde{A} is varied from 0.1 to 10. Generally, $\langle \tilde{v} \rangle$ becomes larger and the range of \tilde{v}_0 that gives finite $\langle \tilde{v} \rangle$ becomes wider as \tilde{A} is increased. For example, the maximum velocity exceeds $\langle \tilde{v} \rangle \approx 7$ and the maximum efficiency can be as large as $\eta_{\text{int}} \approx 0.74$ when $\tilde{A} = 10$. Hence, the strength of active fluctuation has a significant effect on the performance of the I-OUIS, and it can also control the swimming efficiency.

To discuss the efficiency η_{int} of the I-OUIS model more quantitatively, we separately plot dimensionless $\dot{\sigma}_v$, \dot{I} , and \dot{W}_u in fig. 4 as a function of $\tilde{\tau}_m$ when $\tilde{A} = 10$ (corresponding to the purple data in fig. 3(c)). For small $\tilde{\tau}_m$, \dot{I} is larger than \dot{W}_u , whereas \dot{W}_u becomes larger when $\tilde{\tau}_m > 0.5$. However, \dot{I} becomes larger than \dot{W}_u for large $\tilde{\tau}_m$ values. The contribution of $\dot{\sigma}_v$ takes a maximum value at around $\tilde{\tau}_m \approx 1$. As a result, the efficiency is maximized with a value $\eta_{\text{int}} \approx 0.74$ at around $\tilde{\tau}_m \approx 3.6$ as shown in fig. 3(c) (the purple data). A similar behavior can also be seen for $\tilde{A} = 1$ and 5, as presented in figs. S6(a) and (b) in the SM, respectively. From these results, we find that the contribution of \dot{W}_u becomes larger as \tilde{A} is increased.

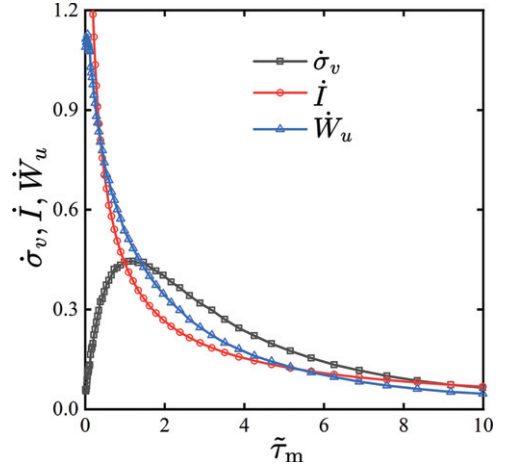


Fig. 4: Contributions of dimensionless $\dot{\sigma}_v$, \dot{I} , and \dot{W}_u to the efficiency η_{int} of the I-OUIS model (see eq. (17)) as a function of $\tilde{\tau}_m$. The choice of parameters corresponds to that of $\tilde{A} = 10$ (purple) in fig. 3(c).

If we do not include \dot{W}_u in the denominator of η_{int} in eq. (17) and simply estimate η_{ext} in eq. (10), the latter can exceed unity for certain choices of the model parameters. A similar situation was reported for an information engine in a non-equilibrium bath [29] that shows an efficiency larger than unity [30] (called “pseudo-efficiency” [31]). To be consistent with the extended second law of thermodynamics with information [18], it is necessary to consider the active power \dot{W}_u resulting from the driving velocity.

Discussion. – For both E-OUIS and I-OUIS models, we have assumed that the measurement and feedback control cause no energy dissipation, and these swimmers acquire net locomotion without any external energy input. On the other hand, the memory spaces of these OUISs are sufficiently large so that the stored information entropy can increase monotonically. Owing to the latter

assumption, the second law of thermodynamics is not violated even though these models can achieve a nonzero velocity under noisy conditions. For the I-OUIS model, the second law can be stated as $\eta_{\text{int}} \leq 1$ or $\dot{\sigma}_v - \dot{W}_u \leq \dot{I}$, which is equivalent to that discussed in the context of information thermodynamics [18]. Notice that the active power \dot{W}_u vanishes in the E-OUIS model. We emphasize again that the maximum efficiency can be obtained by tuning the measurement time τ_m for both OUIS models.

In the two OUIS models discussed in this letter, not only the information but also the particle's inertia (characterized by the mass M) plays an essential role. In the presence of inertia, the unidirectional motion of the particles is maintained and serves as a memory effect. Since we chose $\alpha_1 > \alpha_2$ and $\beta_1 > \beta_2$ for the E-OUIS and I-OUIS models, respectively, the inertia effect is weak when $v < v_0$ and it is strong when $v > v_0$. Since the state with weak inertia can be partially converted to that with strong inertia owing to the switching mechanism, nonzero center-of-mass velocity v can be maintained by positive feedback. The bimodal asymmetric velocity distributions $P(v)$ shown in figs. 1(a) and 2(a) originate from the superposition of a Gaussian distribution reflecting the weak inertia case ($v < v_0$) and a biased distribution reflecting the strong inertia case ($v > v_0$). A similar bimodal velocity distribution was also reported in ref. [17].

Corresponding to the I-OUIS, we give some numbers for the model parameters. Recently, the run-and-tumble motion of *E. coli* has been quantitatively measured by using intermediate scattering functions and the renewal theory [22,23]. For a wild-type *E. coli*, the running and tumbling times were estimated to be $\tau_R = 2.39$ s and $\tau_T = 0.38$ s, respectively, and the average self-propulsion velocity was $u_0 = 15.95 \mu\text{m/s}$. If we identify τ_R as the persistence time τ_a in our OUIS models, the strength of active fluctuation can be estimated as $A \approx 4 \times 10^{-10} \text{ m}^2/\text{s}$. Since the ratio β_1/β_2 can also be estimated from the ratio $\tau_R/\tau_T \approx 6$, the choice $(\beta_1, \beta_2) = (10, 1)$ in fig. 2 is realistic for a wild-type *E. coli*. Experimentally, the running and tumbling times can be controlled by adding a chemical inducer [22,23].

In this work, we have implemented a process of measurement and feedback control in an AOUP. However, the concept of information swimmer is more general. For example, Kumar *et al.* proposed a Brownian inchworm model of a self-propelled elastic dimer [32,33]. In their model, the crucial mechanism is the position-dependent friction coefficients of the two particles. Although such a mechanism was not regarded as an explicit feedback control operation, the proposed Brownian inchworm model offers a typical example of informational active matter [34]. Currently, we are constructing a general framework of information swimmers using the statistical formulation of Onsager-Machlup variational principle [35].

Summary. – In this letter, we have performed numerical simulations of the information swimmers based on the

active Ornstein-Uhlenbeck model; E-OUIS with external feedback control and I-OUIS with internal feedback control. Both OUIS models exhibit nonzero average velocities in the steady state, and their statistical properties as well as the efficiencies have been discussed. For both models, maximum efficiency can be obtained by tuning the measurement time, and hence the information entropy plays an essential role in their locomotion. Depending on the choice of the model parameters, I-OUIS can achieve a larger average velocity and higher efficiency than those of E-OUIS when the active fluctuation is large. Our models provide an important step toward understanding informational transport in biological systems.

We thank Y. HOSAKA for the useful discussions. ZH and SK acknowledge the support by the National Natural Science Foundation of China (Nos. 12104453, 12274098, and 12250710127). SK acknowledges the startup grant of Wenzhou Institute, University of Chinese Academy of Sciences (No. WIUCASQD2021041). KY and SK acknowledge the support by the Japan Society for the Promotion of Science (JSPS) Core-to-Core Program “Advanced core-to-core network for the physics of self-organizing active matter” (No. JPJSCCA20230002). ZH and ZZ contributed equally to this work.

Data availability statement: All data that support the findings of this study are included within the article (and any supplementary files).

REFERENCES

- [1] MARCHETTI M. C., JOANNY J. F., RAMASWAMY S., LIVERPOOL T. B., PROST J., RAO M. and SIMHA R. A., *Rev. Mod. Phys.*, **85** (2013) 1143.
- [2] HOSAKA Y. and KOMURA S., *Biophys. Rev. Lett.*, **17** (2022) 51.
- [3] ROMANCZUK P., BÄR M., EBELING W., LINDNER B. and SCHIMANSKY-GEIER L., *Eur. Phys. J. ST*, **202** (2012) 1.
- [4] UHLENBECK G. E. and ORNSTEIN L. S., *Phys. Rev.*, **36** (1930) 823.
- [5] MARTIN D., O'BYRNE J., CATES M. E., FODOR É., NARDINI C., TAILLEUR J. and VAN WIJLAND F., *Phys. Rev. E*, **103** (2021) 032607.
- [6] TEN HAGEN B., VAN TEEFFELSEN S. and LÖWEN H., *J. Phys.: Condens. Matter*, **23** (2011) 194119.
- [7] NAJAFI A. and GOLESTANIAN R., *Phys. Rev. E*, **69** (2004) 062901.
- [8] YASUDA K., HOSAKA Y. and KOMURA S., *J. Phys. Soc. Jpn.*, **92** (2023) 121008.
- [9] GOLESTANIAN R. and AJDARI A., *Phys. Rev. E*, **77** (2008) 036308.
- [10] HOWSE J. R., JONES R. A. L., RYAN A. J., GOUGH T., VAFABAKHSH R. and GOLESTANIAN R., *Phys. Rev. Lett.*, **99** (2007) 048102.
- [11] YASUDA K., HOSAKA Y., SOU I. and KOMURA S., *J. Phys. Soc. Jpn.*, **90** (2021) 075001.

- [12] LI J., ZHANG Z., HOU Z., YASUDA K. and KOMURA S., *Phys. Rev. E*, **110** (2024) 044603.
- [13] VANSADERS B., FRUCHART M. and VITELLI V., arXiv:2302.07402.
- [14] TOYABE S., SAGAWA T., UEDA M., MUNHEYUKI E. and SANO M., *Nat. Phys.*, **6** (2010) 988.
- [15] PANERU G., DUTTA S., SAGAWA T., TLUSTY T. and PAK H. K., *Nat. Commun.*, **11** (2020) 1012.
- [16] PANERU G., DUTTA S. and PAK H. K., *J. Phys. Chem. Lett.*, **13** (2022) 6912.
- [17] HUANG C., DING M. and XING X., *Phys. Rev. Res.*, **2** (2020) 043222.
- [18] PARRONDO J. M. R., HOROWITZ J. M. and SAGAWA T., *Nat. Phys.*, **11** (2015) 131.
- [19] SERRELI V., LEE C.-F., KAY E. R. and LEIGH D. A., *Nature (London)*, **445** (2007) 523.
- [20] HWANG W. and KARPLUS M., *Proc. Natl. Acad. Sci. U.S.A.*, **116** (2019) 19777.
- [21] TKAČIK G. and BIALEK W., *Annu. Rev. Condens. Matter Phys.*, **7** (2016) 89.
- [22] KURZTHALER C., ZHAO Y., ZHOU N., SCHWARZ-LINEK J., DEVAILLY C., ARLT J., HUANG J.-D., POON W. C. K., FRANOSCH T., TAILLEUR J. and MARTINEZ V. A., *Phys. Rev. Lett.*, **132** (2024) 038302.
- [23] ZHAO Y., KURZTHALER C., ZHOU N., SCHWARZ-LINEK J., DEVAILLY C., ARLT J., HUANG J.-D., POON W. C. K., FRANOSCH T., MARTINEZ V. A. and TAILLEUR J., *Phys. Rev. E*, **109** (2024) 014612.
- [24] CAPRINI and MARCONI U. M. B., *J. Chem. Phys.*, **154** (2021) 024902.
- [25] NGUYEN G. H. P., WITTMANN R. and LÖWEN H., *J. Phys.: Condens. Matter*, **34** (2022) 035101.
- [26] GARCÍA-GARCÍA R., COLLET P. and TRUSKINOVSKY L., *Phys. Rev. E*, **100** (2019) 042608.
- [27] DOI M., *Soft Matter Physics* (Oxford University Press) 2013.
- [28] KLOEDEN P. E. and PLATEN E., *Numerical Solution of Stochastic Differential Equations* (Springer) 1992.
- [29] DI LEONARDO R., ANGELANI L., DELL'ARCIPRETE D., RUOCCO G., IEBBA V., SCHIPPA S., CONTE M. P., MECARINI F., DE ANGELIS F. and DI FABRIZIO E., *Proc. Natl. Acad. Sci. U.S.A.*, **107** (2010) 9541.
- [30] SAHA T. K., EHRLICH J., GAVRILOV M., STILL S., SIVAK D. A. and BECHHOEFER J., *Phys. Rev. Lett.*, **131** (2023) 057101.
- [31] DATTA A., PIETZONKA P. and BARATO A. C., *Phys. Rev. X*, **12** (2022) 031034.
- [32] KUMAR K. V., RAMASWAMY S. and RAO M., *Phys. Rev. E*, **77** (2008) 020102(R).
- [33] BAULE A., KUMAR K. V. and RAMASWAMY S., *J. Stat. Mech.* (2008) P11008.
- [34] LI J., ZHANG Z., HOU Z., HOSAKA Y., YASUDA K., HE L. and KOMURA S., arXiv:2502.20752.
- [35] YASUDA K., ISHIMOTO K. and KOMURA S., *Phys. Rev. E*, **110** (2024) 044104.